TEPES
TURKISH JOURNAL OF
ELECTRICAL POWER
AND ENERGY SYSTEMS

TEPES, Vol. 3, Issue. 2, 90-96, 2023 **DOI:** 10.5152/tepes.2023.23010

RESEARCH ARTICLE

Design and Implementation of a Power Supply for KNX Protocol

Handan Solmaz Akar[1], Erdem Akboy[2], Yılmaz Eyidoğan[1]

[1]Optimus Doruk Elektrik Elektronik Otomasyon San. Tic. A.Ş, İstanbul, Turkey
[2]Department of Electrical Engineering, Yıldız Technical University Faculty of Electrical and Electronics Engineering, İstanbul, Turkey

Cite this article as: H. Solmaz Akar, E. Akboy and Y. Eyidoğan, "Design and implementation of a power supply for KNX protocol," *Turk J Electr Power Energy Syst.*, 2023; 3(2), 90-96.

ABSTRACT

KNX is a widely used organization in the world that standardizes the open system communication protocol for smart home and building automation. KNX controls integrated functions such as heating, cooling, ventilation, lighting systems, audio and video services, security, and energy management in all types of residential, commercial, and industrial building structures. KNX power supply is designed to ensure the continuous operation of these automation systems by considering the number of devices connected to the system. According to the KNX standards, in devices that are compliant with these standards, the main current and communication signals required for the operation of the devices use the same line. Conventional power supplies cannot cope with these standards and therefore special power supplies are required. In this study, a high-frequency (100 kHz) and high-efficiency (minimum 85%) flyback converter-based power supply with 155–265 V_{AC} input and 30 V 640 mA output values in accordance with KNX standards has been designed and implemented.

Index Terms—DCM operation, flyback converter, KNX power supply

I. INTRODUCTION

The KNX protocol has emerged with the combination of European Installation Bus (EIB), European Home Systems (EHS), and Batibus protocols which are developed by the leading automation companies in Europe. Batibus is widely used in Italy, Spain, and France, while EIB is widely used in Germany, German-speaking countries, and Northern Europe. EHS is preferred by digital household and electronic device manufacturers. Nowadays, devices that are compliant with KNX are widely used in many countries of the world and they are under the supervision of the KNX organization [1–9].

The KNX protocol is open source, can be easily integrated into different systems, requires minimal maintenance, and is a problem-free system. For this reason, it is preferred in many projects in industrial and commercial applications. In a project prepared with the KNX protocol, many different brands and product groups that support this protocol can be used together without being dependent on a single manufacturer and brand [2–5].

Nowadays, with the development of technology, the usage of devices that make our daily lives easier and energy consumption have increased. In smart home and building systems, various automation systems are used to meet heating, cooling, lighting, energy management, and other user requirements in terms of both comfort and efficient energy use. KNX organization is widely used in these systems due to its advantages [6–8].

According to the standards of the KNX protocol, in devices connected to this protocol, the main current required for the operation of the device and the communication signals use the same line. Conventional power supplies cannot cope with these standards and therefore special power supplies are required. For this purpose, the KNX power supplies are designed to operate under a wide input range and 30 V_{dc} output voltage. It provides both power and communication transfer on the same line. An integrated choke is used to separate the power supply and communication signals [4–9].

In this paper, a high frequency (100 kHz), high efficiency (minimum 85%) flyback converter-based KNX power supply with 30 V_{dc} output voltage and 640 mA nominal output current, 155–265 V_{AC} input voltage range has been designed and implemented. The losses are reduced and efficiency is increased by using proper snubber cells.

II. FLYBACK CONVERTER

The conventional flyback converter circuit scheme is given in Fig. 1. In this figure, V_{dc} is the input voltage, I_p is the primary current, I_s is the secondary current, Q is the switch, D is the diode, L_p is the primary winding, L_s is the secondary winding, C is the output capacitor, and R is the load.

Received: March 13, 2023
Revision Requested: April 5, 2023
Last Revision Received: April 14, 2023
Accepted: April 20, 2023
Publication Date: June 23, 2023

Corresponding author: Handan Solmaz Akar, handan.solmaz@optimusdoruk.com

Content of this journal is licensed under a Creative Commons Attribution-NonCommercial 4.0 International License.

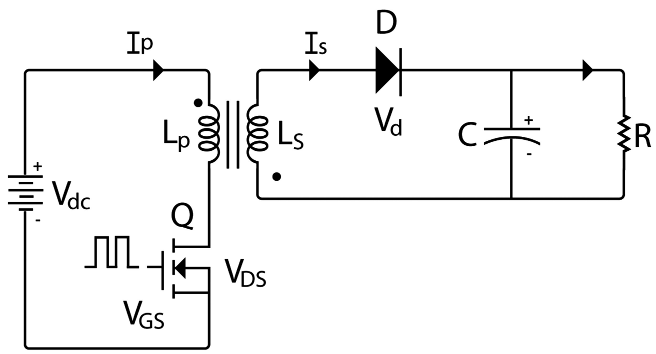

Fig. 1. The conventional flyback converter scheme [10].

The operation of the flyback converter consists of two stages according to the switch states. When the switch is on state, the diode is off state depending on the direction of the voltage which is reflected to the secondary winding of the transformer. The magnetizing inductance is equal to the primary inductance. The input voltage V_{dc} is applied to the magnetizing inductance, and magnetizing current increases, linearly. In this interval, the input energy is transferred to the primary inductance and the load is fed from the output capacitor. When the switch is off state, the diode is turned on, and reflected output voltage is applied to the magnetizing inductance. So, the magnetizing current decreases, linearly, and the magnetizing energy is transferred to the output through the secondary winding [10–16].

Since, the main current is equal to the magnetizing current, the flyback transformer is designed with the air gap. However, the air gap results in leakage inductance and additional voltage stresses. These disadvantages can be overcome using proper snubber cells. For this reason, flyback converters are preferred for low-power applications [10–12].

Flyback converters may operate in discontinuous current mode (DCM) or continuous current mode (CCM) according to the current of magnetizing inductance as shown in Fig. 2. In CCM operation, the magnetizing current does not decrease to zero during the switching period. So, the energy transfer is continuous. Therefore, it is preferred in high-power applications. In DCM operation, the magnetizing current falls to zero and remains at zero for a time during the switching period. The current stress of the switch and electromagnetic interference (EMI) is higher than CCM operation [13–15]. However, DCM operation provides higher efficiency than CCM operation in low-power applications due to no reverse recovery loss of the secondary diode and zero current switching of the MOSFET and secondary diode. Moreover, DCM operation provides advantages

Main Points

- Designed KNX power supply is a high frequency (100 kHz), high efficiency (minimum 85%) flyback converter-based.
- Output voltage has low ripple.
- Oscillations in the KNX power supply are suppressed by snubber cells.

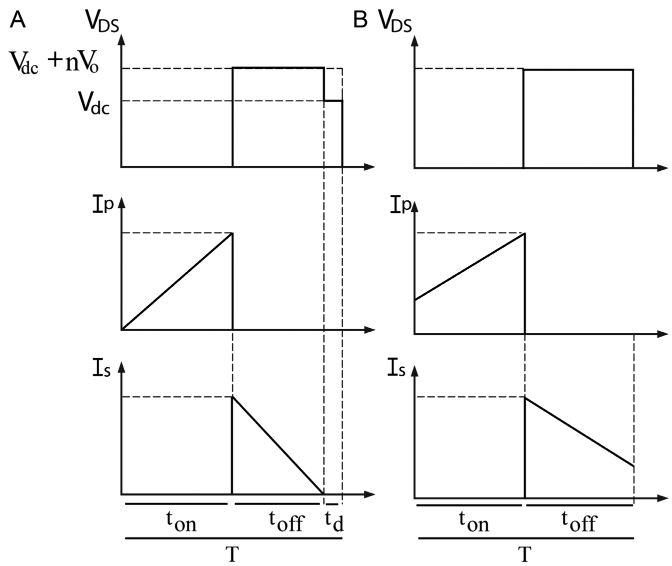

Fig. 2. Typical flyback converter. (a) DCM operation. (b) CCM operation [10].

such as ease of control, small core, fast response, and soft switching in low-power converters.

III. KNX POWER SUPPLY DESIGN

Fig. 3 shows the circuit scheme of the flyback converter-based power supply which is designed for KNX standards. Here, EMI filter, bridge diode, and C_i filter capacitor are used at the input and choke is used at the output. Also, the leakage inductance of the transformer and the parasitic capacitor of the diode are taken considered. Therefore, the RCD snubber is connected ‘parallel’ to the primary winding and the RC snubber is connected parallel to the diode, and the RC snubber is connected parallel to the MOSFET. V_{DS} voltage of the MOSFET increases up to 600 V and the maximum current flowing through the MOSFET while it is in on state is 1.4 A. Therefore, NCP11187 control IC is chosen. This IC integrates 800 V Super junction MOSFET [9].

In the control circuit of the proposed KNX power supply, conventional Pulse Width Modulation is used with output voltage and output current feedback. In KNX power supplies, the voltage range and current values specified in the standard should not be exceeded. Therefore, two compensators for fixed voltage and limited current are used for feedback purposes in the control circuit, as shown in Fig. 3. The oscillations of the feedback voltage cause instability in the power supply control IC. Moreover, these oscillations cause additional oscillations at the switching frequency. To prevent these oscillations, a compensation circuit is established with R1-C1 and R2-C2 components, as shown in Fig. 3 [9].

A. Input Capacitor Design

In flyback converters, the filter capacitor used after the bridge diode in the input part is designed to allow the input voltage to oscillate at a certain rate. In the literature, the value of this capacitor is chosen to be 2–3 µF per W [12]. At the proposed KNX power supply, the output voltage is 30 V, the maximum current is 1.4 A, and the output power

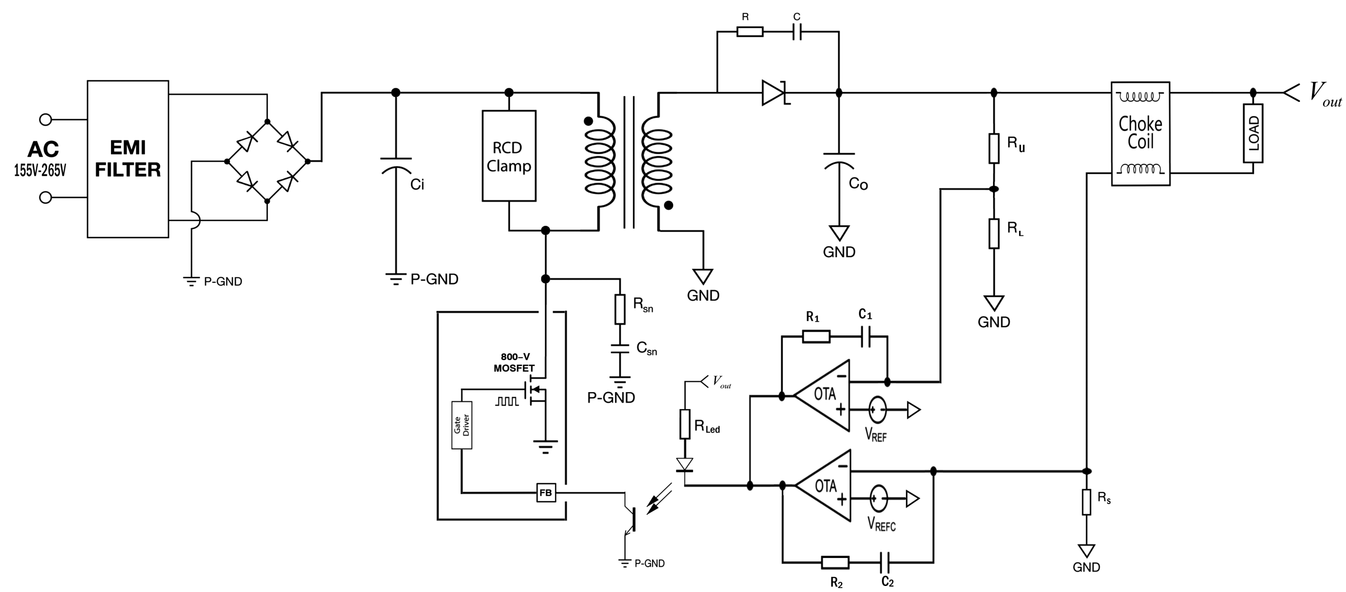

Fig. 3. Flyback converter circuit scheme designed for KNX standards.

is 42 W. Therefore, the input filter capacitor is calculated as 100 µF. The minimum DC input voltage value formula is given as follows:

$$V_{dc\_min} = \sqrt{V_p^{\,2} - 2P_{in}t\frac{1}{C_i}} \tag{1}$$

The minimum input voltage (V_{dc_min}) is calculated using the formula and measured as 109.7 V. Simulation result is performed based on the selected capacitor value and the given formula is presented for 90 V_{AC} in Fig. 4.

According to the 2.7.7 Testing of Power Supply Unit's (PSU) Hold-Up Time test of the KNX Standard "Basic and System Components/Devices - Minimum Requirements," if the mains voltage is interrupted for less than 100 ms, the output voltage should not decrease more than 5%. Thus, in the Hold Up Time test in the proposed power supply, the time elapsed from the moment when the mains voltage is interrupted to the point where the output voltage drops below 95% is measured while the system is operating. The minimum operating voltage of the system

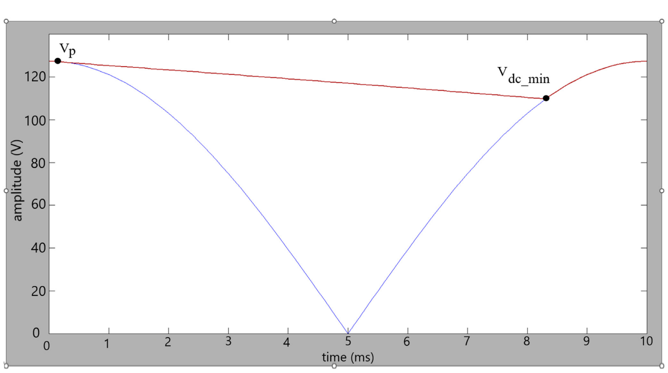

Fig. 4. V_{dc} voltage waveform simulation results.

is determined according to KNX requirements by measuring this interval under different main voltages. According to this requirement, the minimum supply voltage of the KNX Power Supply is measured to be 155 V_{AC} [9].

B. Transformer Design

The transformer design of the converter is performed considering the worst conditions (minimum input voltage and maximum duty cycle). Therefore, the formula for the magnetizing inductance is given as follows [12].

$$L_M = \frac{\left(V_{DC\_min}D_{max}\right)^2}{2P_{in}f_s} \tag{2}$$

Herein, P_{in} is the input power, f_s is the switching frequency. In DCM operations, the required maximum duty cycle D_{max} is chosen 0.5 for the circuit to operate at the worst conditions. Thus, in the proposed design, the magnetizing inductance is calculated as 599 µH for the input power is 25.1 W, V_{DC_min} 109.7 V, f_s 100 kHz, and D_{max} 0.5 [9].

In flyback converters, the current flowing through the switch during turn-on is equal to the magnetizing current. This current depends on the input voltage, and it increases linearly [10–13].

$$i_{LM} = i_{ds} = \frac{V_{dc}}{L_m}t \tag{3}$$

The maximum primary current of the converter is calculated as 0.93 A by considering the worst conditions. In this case, the required number of turns to avoid the saturation of the transformer is calculated depending on the following formula [9].

$$N_p = L_M\frac{i_{DS\_max}}{B_{sat}A_e} \tag{4}$$

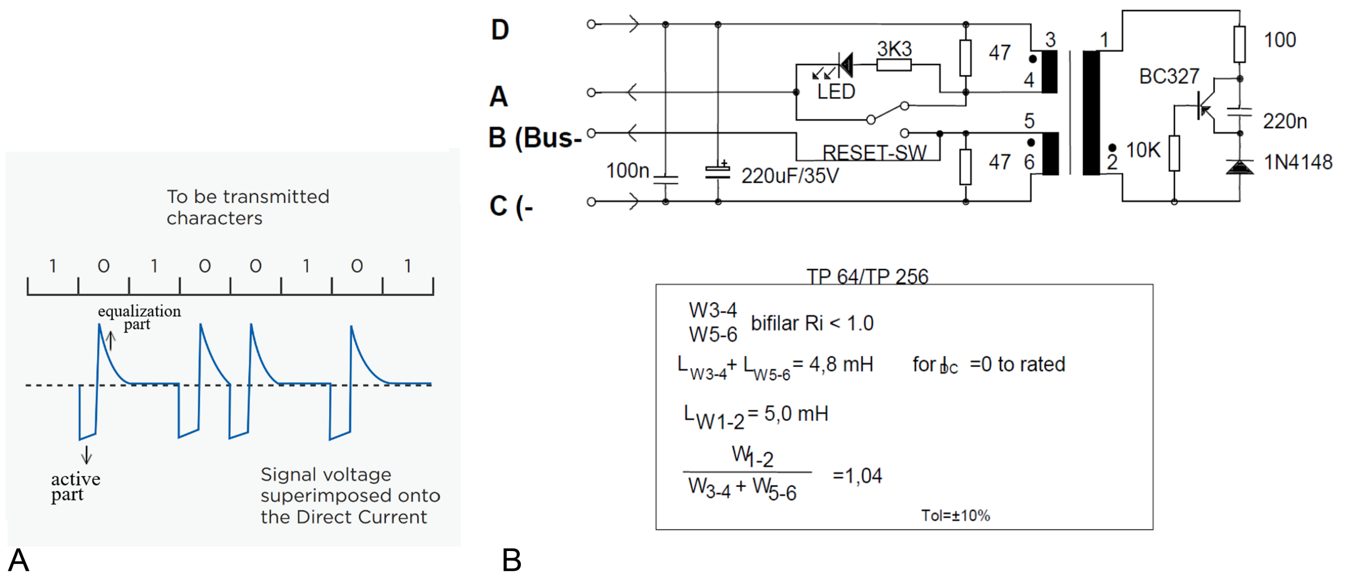

Fig. 5. (a) Signal shape in KNX system. (b) Electrical circuit of a choke module.

Here, B_{sat} is the saturation value of magnetic flux density for ferrite cores, and it is defined as 0.3 Tesla. A_e is the effective area of the core. In this paper, EF25 type core is selected with A_e is 52.5 mm^2. Thus, the number of primary turns is calculated as 53 according to (4) [9].

The turns ratio (n) of the transformer is calculated by using the value of the voltage reflected from the secondary to the primary and the voltage stress of the switch. When n is selected high, the voltage stress value of the switch increases, and when it is selected low, the circuit does not operate properly. For this purpose, n is calculated according to the following formula [12, 16].

$$n = \frac{V_r}{V_o + V_{diode}} \tag{5}$$

Here, V_r is the reflected voltage, V_o is the output voltage, and V_{diode} is the forward voltage of the diode. In these calculations, the forward voltage of the diode is taken as 0.5V. Thus, the value of n is calculated as 3.

C. The Calculation of the Output Capacitor

In the application notes of the switch-mode power supply control IC (NCP11187), it is recommended to determine the output capacitor as 100 µF per 100 mA. Since the current of the designed power supply is nominal 0.711 A, the capacitance value is determined as a minimum of 720 µF. At the same time, according to the KNX requirements, the output voltage ripple value should be less than 100 mV. Therefore, the Equivalent Series Resistance (ESR) value of the selected capacitance should be less than 15 mΩ.

IV. CHOKE COIL DESIGN

In the KNX system, the most common communication for KNX installations is provided by twisted pair data cable. The twisted pair data bus cable provides both data and power to all devices. The data transfer rate is 9600 bits/s (104 µs). The logic zero consists of two parts: an active pulse and an equalization pulse as shown in Fig. 5(a). The voltage falls for a short time and then increases again after a maximum of 104 µs to equalize the original voltage. This is due to the inductor effect of the choke. During the equalization part of the choke coil, it restores the energy used in the active part of the 0-bit. In the case of logic one, the DC voltage level is 30 V [7].

The circuit which is shown in Fig. 5(b) is used in the choke coil design according to the Clause 5 TP1 Choke section of the KNX Standard "Basic and System Components/Devices - Minimum Requirements." The choke shall be designed as electrically symmetrical to improve noise immunity and decrease radiation on the bus [5].

V. EXPERIMENTAL RESULTS

The experimental circuit parameters determined by considering the design criteria of the proposed converter are given in Table I.

TABLE I.
CIRCUIT PARAMETERS

Parameter	Description	Value
C_i	Input filter capacitor	100 µF
C_o	Output filter capacitor	810 µF
L_o	Output filter inductance	1 µH
L_p	Primary inductance	560 µH
L_s	Secondary inductance	62 µH
L_k	Leakage inductance	4.3 µH
NCP11187	Control IC	—
MUR340	Diode	300 V-3A

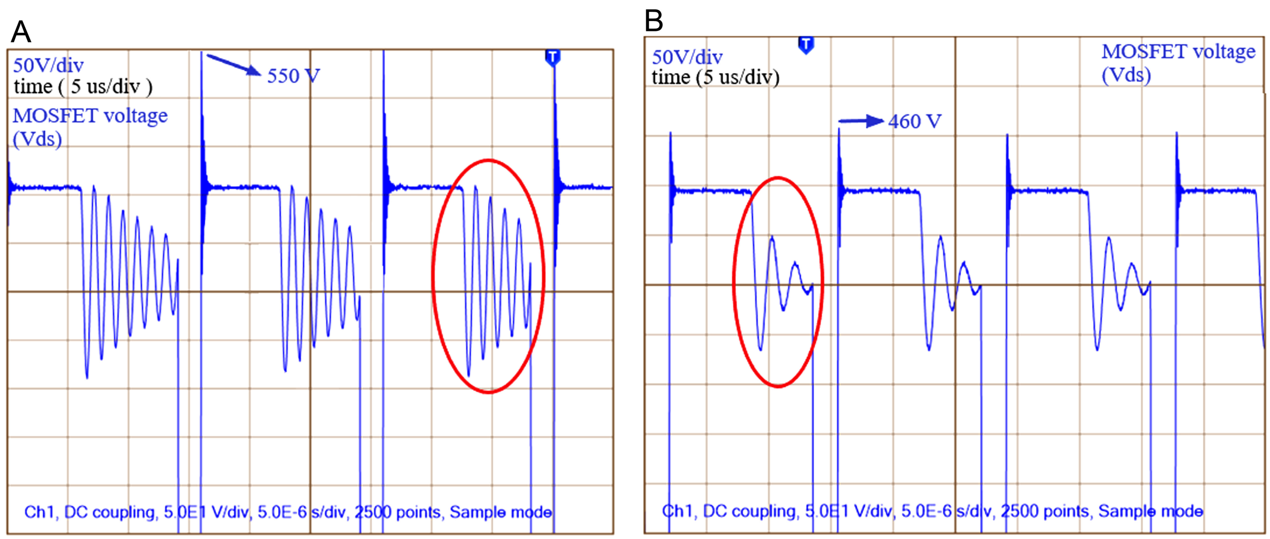

Fig. 6. The voltage stresses of the MOSFET for 220 V RMS: (a) without snubber cell and (b) with snubber cell.

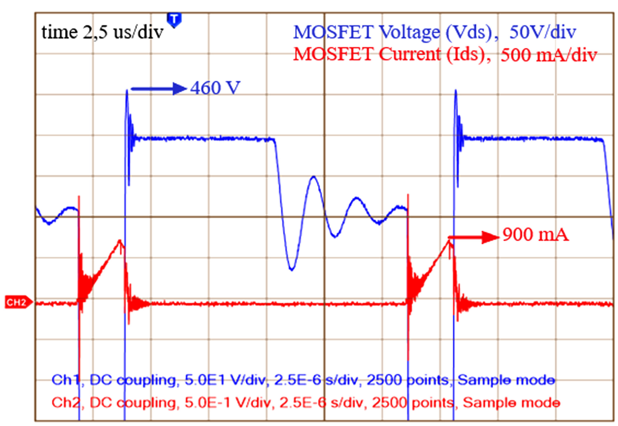

Fig. 7. The voltage and the current waveforms of the MOSFET.

Fig. 6 shows the voltage stresses of the MOSFET for 220 V input voltage. Here in Fig. 6(a), the peak voltages due to leakage inductance in the switch and the oscillations due to the parasitic capacitor of the diode have high values, causing additional losses and noise. In Fig. 6(b), the RCD snubber cell connected to the primary and the RC snubber cell connected to the diode are added to the circuit. It is clear from this figure that oscillations and peak voltages are suppressed successfully.

Fig. 7 shows the voltage and current waveforms in the MOSFET when the input voltage is 220 V_{AC} and the output current is 640 mA. Herein, it is seen that the current increase linearly from zero and provides Zero Current Switching (ZCS).

The output voltage and feedback voltage waveforms are shown in Fig. 8 (a). Here, resistance and capacitance are not used for compensation in the feedback circuit. Therefore, ripples in the feedback

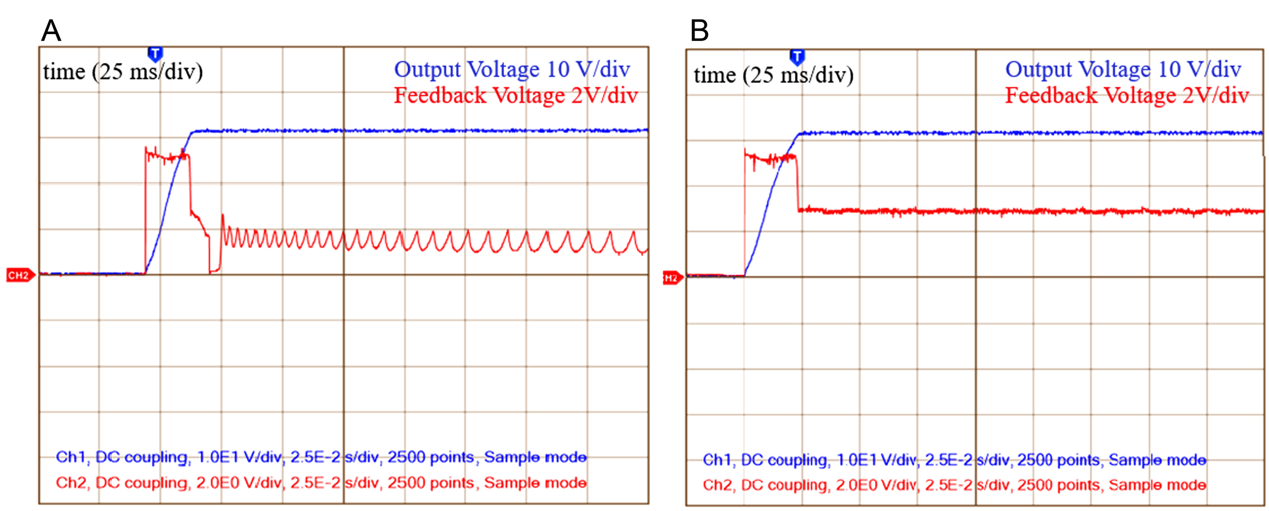

Fig. 8. The output voltage and feedback voltage: (a) with compensation and (b) without compensation circuit in the feedback circuit.

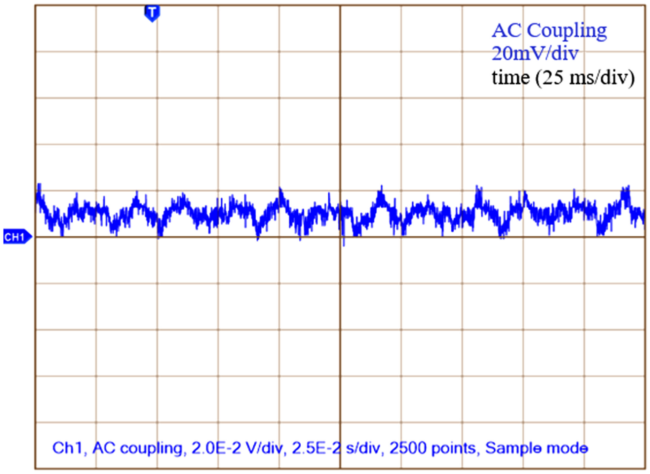

Fig. 9. The ripple waveform of the output voltage.

voltage are clearly visible. In Fig. 8 (b), output voltage and feedback voltage waveforms are shown when a compensation circuit is added to the feedback circuit. It is observed that the ripples in the feedback voltage are suppressed with the added compensation circuit. In Fig. 8, it is seen that the output voltage reaches 30 V in 25 ms. At the same time, there are no overshoot or ripples in the output voltage.

In Fig. 9, the ripples in the output voltage are given taking into account additional compensation components and snubber cells. It is clear that the ripple is around 20 mV, while the output current is 640 mA.

The signal shape during data transferring in KNX is shown in Fig. 10. It can be seen that this signal shape is provided in accordance with KNX standards.

VI. CONCLUSION

KNX Power supplies have 160 mA, 320 mA, 640 mA, 960 mA, and 1280 mA nominal output current options, taking into account voltage and current limitations according to KNX standards. This makes

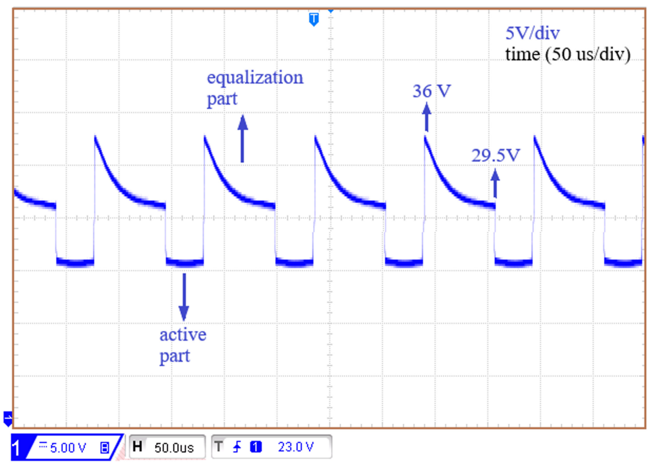

Fig. 10. The data transfer signal in KNX with choke.

KNX power supply special among the others. Moreover, the twisted pair data bus cable provides both data and power to all devices.

The choke is used for data transfer at KNX systems. The special circuit structure at the output line, during the equalization part of the choke, restores the energy used in the active part of the 0-bit, and the efficiency is increased.

Flyback converters are widely used in low-power applications due to their isolation, ease of control, and simple structure. It also provides DCM for soft switching in low-power applications and increases efficiency in converters.

In this paper, a flyback-based power supply in accordance with KNX standards, operating with DCM has been designed and implemented for 155–265 V_{AC} input and 30V 640 mA output values. As a result of the application, output voltage ripple limitations, output current limitations, and data transfer are achieved successfully. Moreover, voltage peaks and oscillations due to leakage inductance are minimized by snubber cells.

Peer-review: Externally peer-reviewed.

Declaration of Interests: The authors have no conflict of interest to declare.

Funding: This study received no funding.

REFERENCES

1. N. Kraus, M. Viertel, and O. Burgert, “Control of KNX devices over IEEE 11073 service-oriented device connectivity,” IEEE Conference on Industrial Cyberphysical Systems (ICPS), Vol. 1. IEEE Publications, Tampere, Finland, 2020, pp. 421–424. [CrossRef]
2. K. Dzierzek, *The Use of KNX/EIB to Control Devices in an Intelligent Home*. Faculty of Mechanical Engineering-Technical University of Košice, Slovakia, 2013.
3. M. Ruta, F. Scioscia, E. Di Sciascio, and G. Loseto, “Semantic-based enhancement of ISO/IEC 14543–3 EIB/KNX standard for building automation,” *IEEE Trans. Ind. Inform.*, vol. 7, no. 4, pp. 731–739, 2011. [CrossRef]
4. I. V. Sita, and P. Dobra, “KNX building automations interaction with city resources management system,” *Procedia Technol.*, vol. 12, pp. 212–219, 2014. [CrossRef]
5. KNX Association, *9/2 Basic and System Components/Devices – Minimum Requirements – Standardised Solutions - Tests KNX System Conformance Testing*, *KNX Standards*, 2022.
6. KNX Association, 4/1 KNX Hardware Requirements and Tests - Environmental, Safety, EMC Requirements, – General, KNX Standards, 2020.
7. KNX Association, *KNX Standarts – The Basics*.
8. M. Y. Toylan, and E. Cetin, “Design and application of a KNX-based home automation simulator for smart home system education,” *Comput. Appl. Eng. Educ.*, vol. 27, no. 6, pp. 1465–1484, 2019. [CrossRef]
9. H. S. AKAR, E. AKBOY, and Y. EYİDOĞAN, “Design and Implementation of a Power Supply for KNX Protocol,” *ELECO 2022 Elektik-Elektronik ve Biyomedikal Mühendisliği Konferansı, ELECO2022*, Bursa, Turkey, November 24-26., 2022, pp. 1-5.
10. N. Coruh, S. Urgun, and T. Erfidan, “Design and implementation of flyback converters,” 5th IEEE conference on industrial electronics and applications, Vol. 2010. IEEE Publications, Taichung, Taiwan, 2010, pp. 1189–1193. [CrossRef]

11. C. Wang, S. Xu, S. Lu, and W. Sun, “A low-cost constant current control method for DCM and CCM in digitally controlled primary-side regulation flyback converter,” *IEEE J. Emerg. Sel. Top. Power Electron.*, vol. 6, no. 3, pp. 1483–1494, 2017. [CrossRef]
12. F. Gökçegöz, E. Akboy, and A. H. Hülya Obdan, “Analysis and design of a flyback converter for universal input and wide load ranges,” *Electrica*, vol. 21, no. 2, pp. 235–241, 2021. [CrossRef]
13. A. A. Saliva, *Design Guide for Off-line Fixed Frequency DCM Flyback Converter. Infineon Technologies North America (IFNa) Corp*, Infenion Design Notes DN2013-01 V1.0, Vol. 16, 2013.
14. S. Howimanporn, and C. Bunlaksananusorn, “Performance comparison of continuous conduction mode (CCM) and discontinuous conduction mode (DCM) flyback converters,” The Fifth International Conference on Power Electronics and Drive Systems, Vol. 2. IEEE Publications, Singapore, 2003, pp. 1434–1438. [CrossRef]
15. T. Zhan, Y. Zhang, J. Nie, Y. Zhang, and Z. Zhao, “A novel soft-switching boost converter with magnetically coupled resonant snubber,” *IEEE Transactions on Power Electronics*, vol. 29, no. 11, pp. 5680–5687.